ALMA memo 548
Performance budget estimation on the ACA system

Hitoshi KIUCHI[a] and Satoru IGUCHI[a]

[a]National Astronomical Observatory of Japan,
2-21-1 Osawa, Mitaka, Tokyo 181-8588, Japan
Reviced on April 4, 2006

ABSTRACT

This memo describes the performance budget estimation on the ACA system.
The most significant thing of interferometer is to maintain the signal coherence. We will discuss the performance budget through the estimation of the signal-to-noise ratio and the signal coherence.

1. SNR OF INTERFEROMETER

The SNR (Signal-to-Noise Ratio) of one baseline interferometer is calculated by Eq. (1)[1]

$$SNR = \frac{\pi}{8k}\frac{S_c\ D_1\ D_2\ \sqrt{\eta_1\ \eta_2}}{\sqrt{T_{s1}\ T_{s2}}}\sqrt{2BT}\rho \tag{1}$$

where

S_c	correlated flux of source,
K	Boltzman's constant,
D_1	the diameter of the antenna (station 1),
D_2	the diameter of the antenna (station 2),
η_1	the antenna *efficiency* of station 1,
η_2	the antenna *efficiency* of station 2,
T_{s1}	the system temperature of station 1,
T_{s2}	the system temperature of station 2,
B	the bandwidth,
T	the integration time.

In the case of SSB, T_s is the same as the system noise temperature: T_{SSB}. And in the case of DSB, however, T_s is the twice of the system noise temperature T_{DSB}.

And signal coherence ρ can be calculated as follow.

$$\begin{aligned}\rho = &(Imperfect\ image\ rejection) \times (Phase\ noise) \times (Imperfect\ band-pass)\\ \times&(Aliasing\ noise) \times (Digitizing) \times (Fringe\ stopping) \times (Fractional\ bit\ correction)\\ \times&(FXFFTnoise) \times (FFTSegmentationloss) \times (Atmospheric\ scintillation).\end{aligned}$$

In this memo, we focus on the coherence ρ estimation.

(Antenna and Frontend efficiency) η is estimated by Sugimoto[2] and the detailed memo will be submitted. The estimated total aperture efficiency is shown in Table 1.

Table 1. Estimated total aperture efficiency, calculated by Sugimoto.[2,3]

Frequency [GHz]	Aperture efficiency of 12 m			Aperture efficiency of 7 m		
	Ant. efficiency	FE efficiency	Total	Ant. efficiency	FE efficiency	Total
94 GHz	79.8 %	97.1 %	77.5 %	76.6 %	97.3 %	74.5 %
136 GHz	79.0 %	97.3 %	76.9 %	76.2 %	97.4 %	74.2 %
200 GHz	77.1 %	94.8 %	73.1 %	75.1 %	94.8 %	71.2 %
224 GHz	77.1 %	93.4 %	72.0 %	75.1 %	93.5 %	70.2 %
289 GHz	74.6 %	92.8 %	69.2 %	73.6 %	92.8 %	68.3 %
404 GHz	65.4 %	93.9 %	61.4 %	67.7 %	93.9 %	63.6 %
670 GHz	50.2 %	92.2 %	46.3 %	57.2 %	92.1 %	52.7 %
860 GHz	35.4 %	88.7 %	31.4 %	45.7 %	88.6 %	40.5 %

Table 2. Estimated system noise temperature in the case of the 25, 50, 75 percentile atmosphere are shown in the Table, calculated by Iguchi.[4]

Frequency [GHz]	DSB system			2SB system		
	25 %	50 %	75 %	25 %	50 %	75 %
94 GHz	30 K	31 K	34 K	45 K	46 K	49 K
136 GHz	38 K	41 K	48 K	58 K	61 K	68 K
200 GHz	61 K	76 K	110 K	89 K	106 K	142 K
224 GHz	60 K	70 K	92 K	91 K	102 K	127 K
289 GHz	96 K	117 K	164 K	150 K	175 K	230 K
404 GHz	222 K	365 K	824 K	315 K	487 K	1036 K
670 GHz	904 K	2640 K	19647 K	1274 K	3571 K	26071 K
860 GHz	1311 K	4438 K	47551 K	1889 K	6178 K	65313 K

(System noise) T_s had been estimated by Iguchi.[4] Estimated T_s, including the system noises from Atmosphere to the Band cartridge, is shown in Table 2.

2. IMPERFECT IMAGE REJECTION

The coherence loss of imperfect image rejection is a loss of cross-talk from the opposite sideband.[5] It is supposed that the output signal is U', the upper side-band of input signal is U, and the lower side-band of the input signal is L. The coupling coefficients are displayed in k, x. Then U' is described as follows:

$$U' = kU + xL \tag{2}$$

The power of the signal is described as follows:

$$< U'^2 >= k^2 < u^2 > +x^2 < L^2 > +2kx < UL > \tag{3}$$

where <> denotes time average

It is supposed that U and L are independent of each other and that they are random noises. Therefore, $< UL >$ is zero. It is restricted by power in uniform, then x is described by $\sqrt{1-k^2}$.

$$U' = kU + \sqrt{1-k^2}L \tag{4}$$

The relationship between k and the image rejection ratio is described as follows:

$$Image\ rejection\ ratio\ [dB] = -10\log(1-k^2) \tag{5}$$

Next, the correlation processing between two stations are considered. The suffixes show each station.

$$\begin{aligned} U_1' &= k_1 U_1 + \sqrt{1-k_1^2} L_1 \\ U_2' &= k_2 U_2 + \sqrt{1-k_2^2} L_2 \end{aligned} \tag{6}$$

The correlated amplitude ρ_{IRM} is

$$\begin{aligned} \rho_{IRM} &= < U_1' U_2' > \\ &= k_1 k_2 < U_1 U_2 > + \sqrt{(1-k_1^2)(1-k_2^2)} < L_1 L_2 > . \end{aligned} \tag{7}$$

The observed data is affected by the Doppler shift caused by the Earth's rotation. This is called "fringe rotation". In this case, the second term $< L_1 L_2 >$ on the right side of the equation becomes zero because fringe rotation is different between the upper sideband and the lower sideband. But $< L_1 L_2 >$ has weak correlation in the case of no fringe rotation (for spectral line observation, in which case $< L_1 L_2 >$ would have no correlation). If the image rejection ratios for two stations are 19.5 dB and 22 dB, k_1 is 0.9944 (image-rejection ratio 19.5 dB) and k_2 is 0.9969 (22 dB). These values are substituted into Eq. (7); then, the coherence loss is calculated as follows:

$$\begin{aligned} 1 - \rho_{IRM} &= 0.87\% : with\ fringe\ rotation \\ &= 0.04\% : without\ fringe\ rotation. \end{aligned}$$

For the purpose of reference, this is not ALMA baseline scheme. If the image rejection ratios for two stations are 10.0 dB and 11 dB without 90 degree phase switching, k_1 is 0.9487 (image-rejection ratio 10.0 dB) and k_2 is 0.9595 (11 dB). In the fringe rotation case, $< L_1 L_2 >$ is no correlation because of the fringe frequencies between $< U_1 U_2 >$ and $< L_1 L_2 >$ are different. The coherence loss is calculated as follows:

$$\begin{aligned} 1 - \rho_{IRM} &= 9.9\% : with\ fringe\ rotation \\ &= 8.2\% : without\ fringe\ rotation. \end{aligned}$$

Therefore, 90-degree phase switching is indispensable operation.

3. PHASE NOISE

We can analyze the behaviors of phase noise, by using the Allan standard deviation[6,7] (commonly called Allan variance). Detailed discussion is described on ALMA memo 530.[10]
Frequency instability refer to a spontaneous and/or environmentally induced frequency change within a given time interval. In other words, frequency instability represents the degree to which the output frequency of a frequency standard remains constant over a given period of time. Since the atomic frequency standard is usually operated as a clock over a long period of time in the time and frequency applications, a measure that can express instability in the short/long term is required to assess the frequency instability. Noises can be classified into five types according to the noise generation mechanism. They are White PM (phase modulation) noise (τ^{-1}), Flicker PM noise (τ^{-1}), White FM (frequency modulation), Flicker FM noise (τ^{0}) and Random walk FM noise ($\tau^{+1/2}$).

3.1. Coherence estimation by Allan standard deviation

The coherence loss caused by the LO phase noise is described in detail in ALMA memo 530.[10]
The fractional loss of coherence due to the instability in the frequency standard for *T-sec* integration times is estimated by Eq. (8).[1,11]

$$L_c = \omega_o^2 [\frac{\alpha_p}{6} + \frac{\alpha_f}{12} T + \frac{\sigma_y^2}{57} T^2] \tag{8}$$

where

Table 3. As only for the white PM noise, the coherence loss is independent during the integration time. However other cases, the coherence loss strongly depends on the integration time. This table shows the Estimated the time-independent loss and the coherent integration time with 5 % and 10 % losses. This loss estimation is calculated at the highest LO frequency of each Band and excludes the atmospheric scintillation loss.

Time independent loss		Time dependent loss		
	Coherence loss Total		Integration time Total system	
Flicker FM	none	Flicker FM	none	2.2×10^{-16}
White FM	none	White FM	4.5×10^{-15}	none
White PM	1.3×10^{-13}	White PM	1.3×10^{-13}	1.3×10^{-13}
108 GHz	0.18%	108 GHz	>10000 sec	>10000 sec
151 GHz	0.28%	151 GHz	>10000 sec	>10000 sec
199 GHz	0.46%	199 GHz	>10000 sec	8480 sec
263 GHz	0.78%	263 GHz	>10000 sec	6305 sec
365 GHz	1.49%	365 GHz	9420 sec	4365 sec
488 GHz	2.65%	488 GHz	4585 sec	3033 sec
708 GHz	5.58%	708 GHz	1365 sec	1623 sec
938 GHz	9.78%	938 GHz	110 sec	280 sec

L_c the loss of coherence,
ω_o the angular frequency of local oscillator,
α_p the Allan variance [$(standard\ deviation)^2$] of white phase noise at 1 sec,
α_f the Allan variance [$(standard\ deviation)^2$] of white frequency noise at 1 sec,
σ_y^2 the constant Allan variance [$(standard\ deviation)^2$] of flicker frequency noise,
T the integration time [sec].

3.2. Estimated coherent integration time cause by system phase instability

In this subsection, we focus on the coherent integration time with $5, 10\%$ coherence loss. The cause of the coherence loss is the system phase instability. During the coherent integration time, the observed phases (a signal phase vector and a noise phase vector) of cross-spectrum are vectors integrated in order to detect a fringe.[12] In the system-level technical requirements of the ALMA project, the instrumental delay/phase error about the total system should be 75 fs in the short-time period, and a drift of 25 fs in RMS integrated difference between 10 sec averages at intervals of 300 sec. We can convert the values to the Allan standard deviation, it is assumed that the noises are in the white PM and the flicker FM. According to the ALMA memo 530, they are 1.3×10^{-13}(White PM) with 2.2×10^{-16} (Flicker FM), or as are 1.3×10^{-13}(White PM) with 4.5×10^{-15} (White FM) in total. These values are gained by calculating the values of ALMA LO/Total and those of short/long term specifications.[19] The calculated coherent integration times are shown in Table 3.

4. FILTERING LOSS

In this section, we consider filtering losses,[5] imperfect filtering and aliasing noise, which are shown in Fig. 1.

4.1. Imperfect band-pass

The loss L_c caused by an imperfect band pass can be estimated by the following equation[1]:

$$L_c = 1 - \frac{1}{\sqrt{1 + 2\sum_{\tau=1}^{N} R_{11}(\tau) R_{22}(\tau)}}, \tag{9}$$

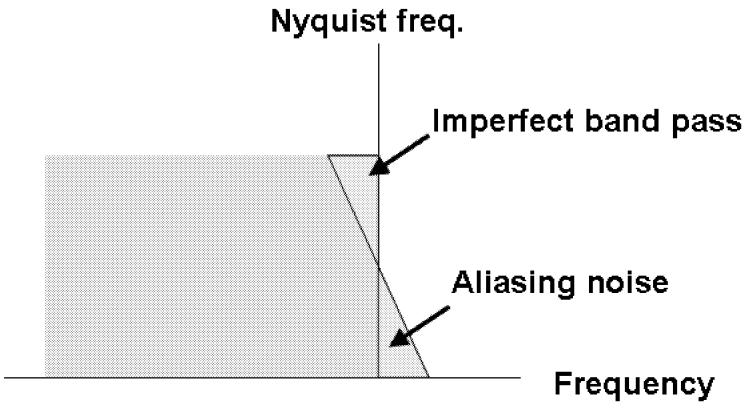

Figure 1. An image of filtering loss.

$R_{11}(\tau)$ *and* $R_{22}(\tau)$ are the auto-correlation functions of correlated functions after the low-pass filters ♯1 and ♯2; N is the number of samples existing in the integration period of τ.

4.2. Aliasing (fold-over) noise

If under sampling occurs, there is a component whose frequency is more than half of the sampling frequency. This is folding over noise. The digitized data has some deformation caused by aliasing noise. The coherence loss is defined by L , and it is calculated as follows[1]:

$$L_c = 1 - \frac{\int_0^{\omega_o} P(\omega)\, d\omega}{\int_0^{2\omega_o} P(\omega)\, d\omega}, \tag{10}$$

where

$P(\omega)$	is the transfer function,
ω_b	is $2\pi f_c$, and
f_c	is *the nominal cutoff frequency of the low-pass filter.*

We do not have the information on band-pass filters. We assume that anti-aliasing filters are composed of 10th-order Butterworth low-pass and high-pass filters. The Butterworth filters are used in VLBI data acquisition terminals. The transfer function of the Butterworth filter is described in the next equation:

$$P(f) = \frac{1}{1 + (\frac{f}{f_d})^{2n}}, \tag{11}$$

where

n	is *the order of the filter, and*
f_d	is *the 3-dB cutoff frequency.*

The cutoff frequency f_d is selected to minimize the coherence loss which is the total loss of the imperfect band-pass and the aliasing noise. The selected value is $f_d = 0.96 \times f_c$ for $n = 10$ (example: $f_d = 0.96 \times f_c$ for $n = 9$, and $f_d = 0.91 \times f_c$ for $n = 7$).
The worst case of coherence loss of the system is as follows:

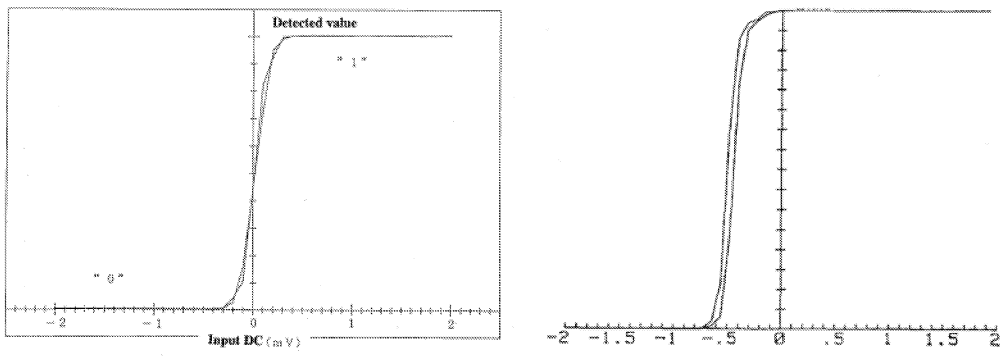

Figure 2. Example of sampling characteristics.

Imperfect band pass	= 0.5% (on each filter n=10),
Aliasing noise	= 1.0% (on each filter n=10).

Other filter types may result in lower loss factors, but have phase characteristics that are more non-linear.

5. DIGITIZING

5.1. Fuzzy digitizing

Analog input IF signals are digitized by A/D converters. There is a region of fuzzy digitizing because of the undetermined digitizing and hysteresis of the A/D converter.[5] Assuming that an input signal has a Gaussian distribution and its mean is zero, the probability of a region of undetermined digitizing is calculated by the following equation.

$$R(V_o) = \int_{V_{oL}}^{V_{oH}} \frac{1}{\sqrt{2\pi}V_e} \exp\left[\frac{-2V^2}{2V_e^2}\right] dV, \tag{12}$$

where

V_{oH}	is *higher voltage in a region of undetermined digitizing, and*
V_{oL}	is *lower voltage in a region of undetermined digitizing, and*
V_e	is *the effective voltage of a signal.*

An example of the sampling characteristics are shown in Fig. 2. Left side of the figure is an ideal case, however the right side of the figure has DC offset and hysteresis property. They are strongly depended on implementation and component mounting. These variations of A/Ds on the antenna lead to coherence loss. We have to consider the worst case.

If the input signal power is 0 dBm, then $V_e = 0.224V$ and it is assumed that $V_{oH} - V_{oL}$ is smaller than 2 mV which is the worst case of the common A/Ds or comparators. The coherence loss calculated with Eq. (18) is less than 0.36%. Next, we discuss the comparator offset. If the probability of a comparated value of "1" from station 1 is $\rho_1(1)$, then

$$\textit{the probability of "1" and "1"} \quad : \quad P_1 = \rho_1(1)\rho_2(1) \tag{13}$$

$$\textit{the probability of "1" and "0"} \quad : \quad P_2 = \rho_1(1)(1-\rho_2(1)) \tag{14}$$

$$\textit{the probability of "0" and "1"} \quad : \quad P_3 = (1-\rho_1(1))\rho_2(1) \tag{15}$$

$$\textit{the probability of "0" and "0"} \quad : \quad P_4 = (1-\rho_1(1))(1-\rho_2(1)), \tag{16}$$

where

$$\rho_1(1) \quad is \quad the\ probability\ of\ "1"\ in\ data\ \sharp 1\ of\ station\ 1,\ and$$
$$\rho_2(1) \quad is \quad the\ probability\ of\ "1"\ in\ data\ \sharp 2\ of\ station\ 2.$$

For P_1 and P_4, the correlation is positive. For P_2 and P_3, the correlation is negative. Thus, the output of the count-bit M is as follows.

$$\begin{aligned} M &= N(P_1 - P_2 - P_3 + P_4) \\ &= N[2(P_1 + P_4) - 1], \end{aligned} \tag{17}$$

where N is the total bit.

The correlated value is

$$\frac{M}{N} = 2(P_1 + P_4) - 1 \tag{18}$$

The calculated coherence loss from Eq. (18) in the worst case of a 2-mV DC comparator offset, is less than 0.052%.

5.2. Quantization loss

It is assumed that the signals are Gaussian random processes. Fortunately, the correlation functions of the signals can be recovered readily from the correlation function of the quantized representations of the signals. The quantization coherence of 3-bit (8-level) is 0.960.[13,14] Therefore the coherence loss is 4.0%.

6. CORRELATION LOSS

6.1. Re-quantization loss

In the FX correlator, 4-bit quantization strain occurs after FFT processing. The worst case of the quantization coherence with 4-bit 16-level is 0.988.[13,14] Therefore the coherence loss is 1.2%.

6.2. Fringe-rotation compensation loss

To compensate for fringe rotation, multiply the cross-correlation function by $\exp(j\omega_f t)$, where ω_f is a frequency of the fringe rotation. In the ALMA system, an $\exp(j\omega_f t)$ signal in analog is used for fringe stopping at the 1st or 2nd local signal. The estimated coherence loss of the fringe rotation is negligible.

6.3. Fractional-bit-correction loss

Another type of coherence loss is a discontinuous delay tracking which is caused by a bit shift in a buffer memory. The loss is due to a fractional bit.

(XF correlation scheme) The frequency of the phase generator usually equal to the fringe rate at the center of the sampled analog signal (RF). This choice minimizes the average SNR loss over a correlation interval. However, in ALMA system, the fringe stopping is performed on the LO frequency in order to perform fringe-stopping on the upper- and lower-sideband signals simultaneously. It is desirable to reference the correlation processing to a frequency at the baseband (equivalent to LO frequency) (Fig. 3). During each period of time for which the delay occurs constantly (during the interval over which the quantized delay error tracks within ± 0.5 sample period) the phase rotator operates at a phase rate corresponding to the fringe rate.
The correlation processor compensates for the fringe phase on the based frequency of the receiving band in the time domain. This fringe phase is not perfectly compensated for the entire bandwidth. The phase uncompensated for is called a "fractional phase", because the edge of the signal band is referenced through overall processing.[15]

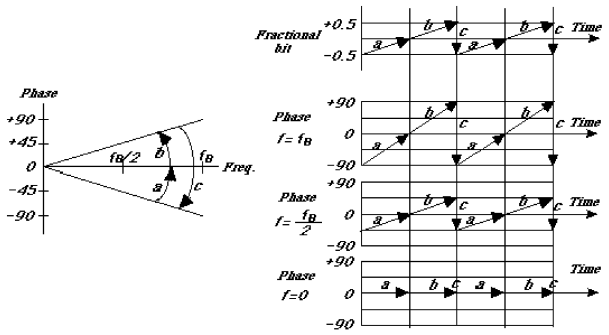

Figure 3. Fringe rotation on the baseband

It is assumed that the sampling period is T_{bit}, signal bandwidth is f_B ($= 1/(2T_{bit})$ in Nyquist sampling), and simple cross-spectrum at f is $X(f) = 1$. The cross-correlation amplitude on delay error from $-T_{bit}/2$ to $T_{bit}/2$, is calculated as:

$$P_A = \int_{-T_{bit}/2}^{+T_{bit}/2} \int_{0}^{f_B} X(f)\, df dt = f_B T_{bit} = \frac{1}{2} \tag{19}$$

In ALMA 2SB system, the fringe stopping is performed by the LO frequency, therefore this scheme is equivalent to the baseband fringe stopping. The changing phase along time is displayed in $\exp(j2\pi ft)$. The obtained cross-correlation amplitude is calculated as follow;

$$\begin{aligned} P_B &= \int_{-T_{bit}/2}^{+T_{bit}/2} \int_{0}^{f_B} X(f) \exp(j2\pi ft)\, df dt \\ &= \frac{1}{\pi} \int_{0}^{+T_{bit}/2} \frac{\sin(2\pi f_B t)}{t}\, dt \\ &= \frac{1}{2}\left(1 - \frac{\pi^2}{2^2 \cdot 3 \cdot 3!} + \frac{\pi^4}{2^4 \cdot 5 \cdot 5!} - \frac{\pi^6}{2^6 \cdot 7 \cdot 7!} + \cdots\right) \end{aligned} \tag{20}$$

$$\begin{aligned} \frac{P_B}{P_A} &= 1 - \frac{\pi^2}{2^2 \cdot 3 \cdot 3!} + \frac{\pi^4}{2^4 \cdot 5 \cdot 5!} - \frac{\pi^6}{2^6 \cdot 7 \cdot 7!} + \cdots \\ &\approx 1 - \frac{\pi^2}{72} \end{aligned} \tag{21}$$

Then, the coherence loss is $\pi^2/72 \approx 13.7\%$. And in the case of 1/8 bit shift which is a baseline plan, we can calculate the coherence loss in analytic, the loss is reduced to $\pi^2/4608 \approx 0.21\%$. This estimation is available on the Nyquist frequency.

(FX correlation scheme)[16] This paragraph, we quote part of Romney's article.[16]
Time domain signals are displayed as follows.

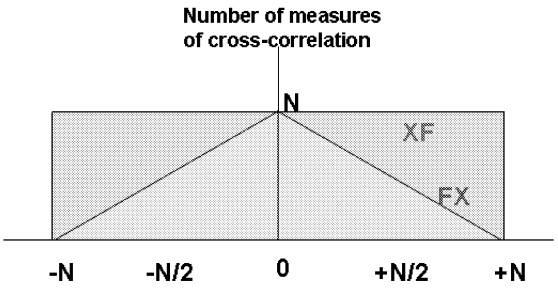

Figure 4. Relative density of lag measurements for lag and FX correlators.

$$X_i(t) = A(t - \epsilon_i) \tag{22}$$
$$Y_j(t) = A(t - \epsilon_j) \tag{23}$$

Where ϵ_i is a fractional bit. The FX correlator output in frequency domain is as follow.

$$S_{ij} = e^{-j2\pi\nu(\epsilon_i - \epsilon_j)} S(\nu) \tag{24}$$

Although the same phase slope arises in both XF and FX architecture, in the FX scheme we can correct the slope at Fourier transform output before cross-multiplication and integration. Applying the correction at this point is equivalent to interpolating the fractional-bit delay. In other words, corrections for discrete delay tracking could be done by applying phase ramps on the FX FFT outputs. The fractional-bit error can be essentially eliminated in an FX correlator. It allows the FX correlator to operate in all case with no fractional-bit loss at all.

6.4. FFT noise[17]

In the ACA FX, the SNR of 16 bit quantization is 85.4 dB (at optimum loading factor) with 11 stages in the FFT. Therefore, the total SNR of FFT is approximately 75 dB, which means 3.2×10^{-8}. This is negligible.

6.5. Segmentation loss[16]

In this subsection, we quote part of Romney's article.[16]
We consider the response of the FX correlator in lag domain. First, transforming data samples in segments of length N yields a range of 2N lags covering. And these lags are heavily tapered by the triangle function; these are fewer pairs of samples within the set of N which can form large lags than small lags. This effect is shown schematically in Fig. 4.
According to this estimation, the maximum segmentation loss is 25%.
For ACA correlator, this loss is true with only the highest resolution (3.8 kHz). The binning reduces the segmentation error. In the case of 128-ch, the binning suppress the loss to 0.2%[17] compared with XF correlator.

6.6. Multi-baseline processing

(Baseline-based delay tracking) Digitized data cannot usually be set precisely to the desired delay, but can always be set to within ± 0.5 sample periods of the desired delay. The dashed line, in Fig. 5, represents the desired delay, but the actual delay can be tracked in a step of the integral sample periods. This results in a saw-tooth "baseline-delay error", a small SNR-coherence loss occurs (less than 4% in 1-bit shift, and negligible in the 1/8-bit shift).

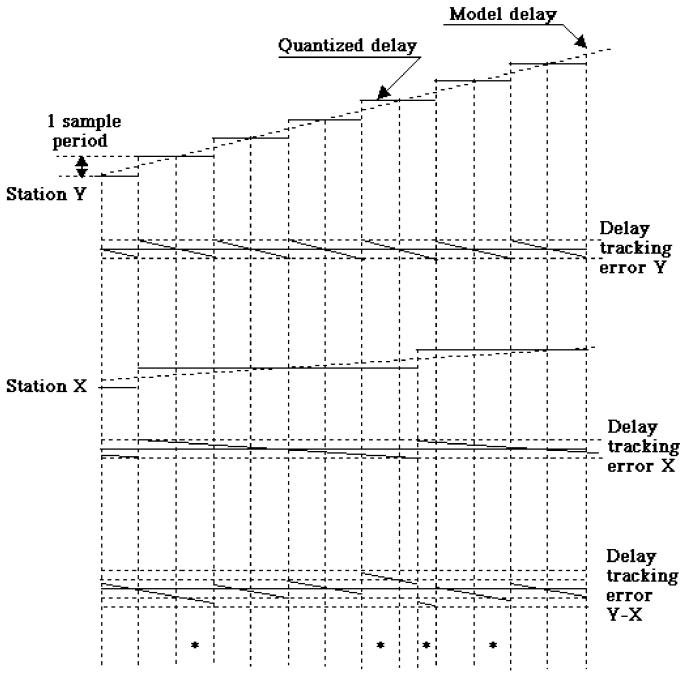

Figure 5. Delay tracking for multi-baseline station-based correlator

(Station-based delay tracking) The X data and Y data are delayed individually with respect to some common reference point, usually the center of the Earth.

The delay error of each station tracks between -0.5 and $+0.5$ sample periods as the delay changes, the baseline delay error will track between -1.0 and $+1.0$ sample periods. This is shown in Fig. 5. Where the Y delay, Y-delay error, X delay and X-delay error for a sample are shown in the upper four traces. Usually, Y- and X-delay errors are independent, representing the uncorrected baseline-delay error is the dashed line in the bottom trace. The uncorrected baseline delay can behave quite peculiarly. The baseline-delay error must be brought within ± 0.5 sample periods. This requires the insertion of a 3-tap shift register that allows the Y delay to be changed by ± 1 sample period. By selecting the appropriate delay of a 3-tap shift register, the baseline error can be suppressed to the solid line.

The SNR loss of the rotator would double once the fringe stopping must be done for both of X and Y data. The rotation waveforms are rough approximations of true cos / sin curves, a fringe rotator generates a set of undesired harmonics in addition to the fundamental-rotation frequency.

One advantage of the FX processor is that the correction for the misalignment of the data streams due to the finite sampling interval can be made easily by adding a linear phase shift to the output of the Fourier transformation of a cross-spectrum.

7. ATMOSPHERIC SCINTILLATION

The stability of the atmosphere has been determined to be about 1×10^{-13} at 100 sec by VLBI.[1,18] However, the atmospheric scintillation might be reduced dramatically at a high-altitude place such as ALMA, and/or by the fast beam switching and the WVR (Water-Vapor Radiometer) correction. After WVR correction,[19,20] it is expected that the phase instability[20] is improved to 8.3×10^{-14}. It's estimated that the stability of Atmospheric scintillation is flicker FM noise and cross over to white PM at 4 seconds in the confirmed space of ACA. Therefore, according to this assumption, the atmospheric scintillation loss is estimated according to Eq. (25), it is shown in Table 4.

Table 4. Assumed stability of atmospheric scintillation is 8.3×10^{-14} or 1.1×10^{-13} in Flicker FM noise, turning over time is 4 seconds. Estimated coherence losses are shown in the Table.

Atmosphere scintillation loss in [%]		
	with WVR	without WVR
Flicker FM	8.3×10^{-14} up to 4 sec.	1.1×10^{-13} up to 4 sec.
White PM	Over 4 sec.	Over 4 sec.
Integration time	100 sec	100 sec
94 GHz	0.11 %	0.19 %
136 GHz	0.23 %	0.40 %
200 GHz	0.49 %	0.85 %
224 GHz	0.61 %	1.07 %
289 GHz	1.02 %	1.78 %
404 GHz	1.99 %	3.49 %
670 GHz	5.46 %	9.59 %
860 GHz	9.00 %	15.81 %

$$L_{atm} = \omega_o^2 [\frac{\sigma_y^2}{57} T^2 + \frac{\alpha_p}{6}] \tag{25}$$

where

L_{atm} the loss of coherence,
ω_o the angular frequency of RF,
α_p the Allan variance [$(standard\ deviation)^2$] of white phase noise at turning over point,
σ_y^2 the constant Allan variance [$(standard\ deviation)^2$] of flicker frequency noise,
T the turning over point [sec].

8. ESTIMATED COHERENCE LOSS

Table 5 shows a summary of coherence loss discussed above. The estimated total coherence loss is about 24% in data-acquisition systems. Then the coherence ρ is estimated as 76%.

9. SNR AND SENSITIVITY ESTIMATION

We estimate the SNR according to Eq. (1), Table 1, Table 2, and Table 6. The results are shown in Table 7.
And the calculated sensitivities are shown in Table 8, and Fig. 6.

10. CONCLUSION

We discuss the main points of signal coherence. The coherence loss is a serious problem in the interferometer. As the coherence loss is related to the signal frequency, it is getting harder than ever to maintain the signal coherence. According to the above discussion, what is the most important thing for keeping coherence is:
Firstly, to suppress the Flicker FM and White FM noises. Secondly, by using WVR, to compensate the atmospheric scintillation in Flicker FM noise better than 1×10^{-13} in mm-wave and 1×10^{-14} in sub-mm-wave. It is clear that the turning over point of atmospheric scintillation is involved coherence deeply.

Table 5. Estimated coherence loss in the worst case of 860 GHz.

Coherence loss factor	Fringe rotation	w/o fringe rotation
Down conversion		
Imperfect image rejection (with 90 deg phase SW)	0.9 %	0.04 %
Phase noise		
White PM(1.3×10^{-13}) and White FM (4.6×10^{-15})	8.4 %	8.4 %
or White PM(1.3×10^{-13}) and Flicker FM (2.2×10^{-16})	or 8.2 %	or 8.2 %
with 100 sec integration time (Total)		
Filtering (assumed 10th Butterworth HPF/LPF)		
Imperfect band-pass (0.5 % on each filter)	1.0 %	1.0 %
Aliasing loss (1.0 % on each filter)	2.0 %	2.0 %
A/D		
Fuzzy digitizing	0.1 %	0.1 %
Quantization (3-bit 8-level)	4.0 %	4.0 %
FX correlator		
Re-Quantization (4-bit 16-level)	1.2 %	1.2 %
Fringe rotation	0.0 %	0.0 %
Fractional bit correction	0.0 %	0.0 %
FFT noise (-75 dB)	0.0 %	0.0 %
Segmentation loss (128-ch binning)	0.2%	0.2%
Multi-baseline (station based)	0.0 %	0.0 %
Total system loss	16.6 %	14.2 %
Atmosphere scintillation		
8.3×10^{-14} (ACA area), 100 sec integration	9.0 %	9.0 %
turning over time is 4 sec.		
Total loss include atmosphere	24.2 %	22.0 %

Table 6. Estimated system coherence with the atmospheric scintillation, integration time is 100 sec and atmospheric scintillation is assumed to 8.3×10^{-14} (Flicker FM, turning over time is 4 sec.) after WVR correction.

	Coherence ρ
RF frequency	100 sec
94 GHz	90.8 %
136 GHz	90.6 %
200 GHz	90.1 %
224 GHz	89.9 %
289 GHz	89.2 %
404 GHz	87.6 %
670 GHz	81.7 %
860 GHz	76.0 %

Table 7. Estimated SNR on one baseline (a pair of antennas).

Atmospheric scintillation is 8.3×10^{-14}, WVR is required.												
25-percentile atmosphere												
Flux density 1 Jy												
100 sec integration												
Using 8 Ifs. Bandwidths are 16 GHz at 2SB mode and 32 GHz at DSB mode.												
	System				Turning over is 4 sec				Turning over is 100 sec			
	SNR of 12 m		SNR of 7 m		SNR of 12 m		SNR of 7 m		SNR of 12 m		SNR of 7 m	
RF [GHz]	2SB	DSB	2SB	DSB	2SB	DSB	2SB	DSB	2SB	DSB	2SB	DSB
94 GHz	1146	1216	375	398	1145	1215	375	397	663	703	217	230
136 GHz	882	952	290	312	880	950	289	312	103	111	34	36
200 GHz	545	562	181	186	542	560	180	185	-	-	-	-
224 GHz	524	562	174	187	521	559	173	185	-	-	-	-
289 GHz	305	337	102	113	302	333	101	112	-	-	-	-
404 GHz	128	128	45	45	125	125	44	44	-	-	-	-
670 GHz	23	23	9	9	22	22	8	8	-	-	-	-
860 GHz	10	10	4	5	9	9	4	4	-	-	-	-

Table 8. Estimated sensitivity on one baseline (a pair of antennas).

Atmospheric scintillation is 8.3×10^{-14}, WVR is required.				
25-percentile atmosphere				
100 sec integration				
Using 8 IFs. Bandwidths are 16 GHz at 2SB mode and 32 GHz at DSB mode.				
Flux density in [mJy]				
	Turning over is 4 sec			
	Sensitivity of 12 m		Sensitivity of 7 m	
RF [GHz]	2SB	DSB	2SB	DSB
94 GHz	0.9	0.8	2.7	2.5
136 GHz	1.1	1.1	3.5	3.2
200 GHz	1.8	1.8	5.6	5.4
224 GHz	1.9	1.8	5.8	5.4
289 GHz	3.3	3.0	9.9	8.9
404 GHz	8.0	8.0	22.7	22.6
670 GHz	46.0	46.1	118.7	119.1
860 GHz	108.1	106.1	246.2	241.7

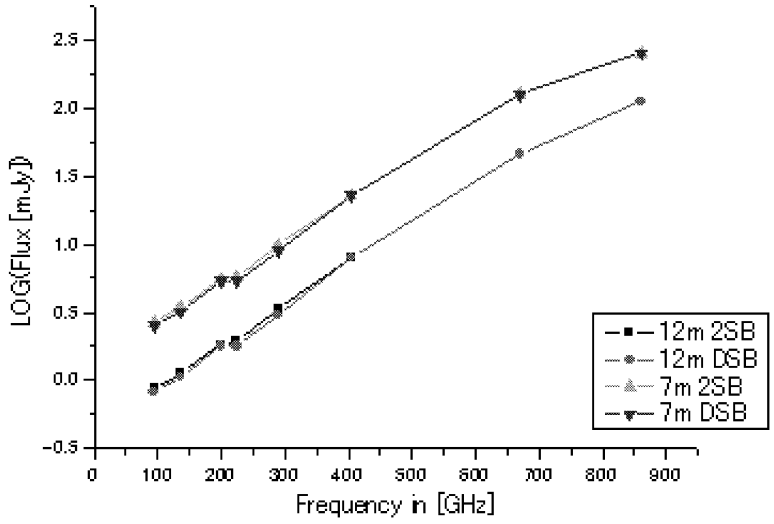

Figure 6. Estimated sensitivity in LOG(Flux [mJy]). Using 8 IFs, Bandwidths are 16 GHz at 2SB mode and 32 GHz at DSB mode. 25-percentile atmosphere, 100 sec integration time.

REFERENCES

1. A.E.E.Rogers and J.M.Moran, "Coherence limits for very-long-baseline interferometry," IEEE Trans. Instrum. Meas., Vol. 30, No. 4, pp. 283-286, Dec. 1981.
2. M.Sugimoto, M.Saito, S.Iguchi, and K.Kimura, "ACA 7m optics analysis," which will be submitted to the ALMA memo.
3. ACA System PDR (ALMA EDM)
4. S.Iguchi," Radio Interferometer Sensitivities for Three Types of Receiving Systems: DSB, SSB, and 2SB Systems," Publ. Astron. Soc. Japan 57, pp643-677, 2005.
5. H.Kiuchi, J.Amagai, S.Hama, and M.Imae," K-4 VLBI data acquisition system," Publ. Astron. Soc. Japan 49, pp699-708, 1997.
6. D.W. Allan, "Statistics of Atomic Frequency Standards," Proc. IEEE 54, 221 (1966).
7. D.W.Allan,"Report on NBS dual mixer time difference system (DMTD) built for time domain measurements associated with phase 1 of GPS," NBS IR 75 827, Jan. 1976.
8. http://ft.nist.gov/
9. http://www.nict.go.jp/
10. H.Kiuchi, "Coherence estimation on the measured phase noise in Allan standard deviation", ALMA memo 530.
11. N.Kawaguchi, "Coherence loss and delay observation error in Very-Long-Baseline Interferometry," J. Rad. Res. Labs., vol.30, no.129, pp.59-87, Mar. 1983.
12. H.Kiuchi, "A highly stable crystal oscillator applied to the VLBI reference clock," IEEE Trans. IM, Vol.45, No.1, pp177-183, 1996.
13. A.R.Thompson,"Quantization efficiency for eight or more sampling levels," ALMA memo 220, Jul. 1998.
14. S.Iguchi and N.Kawaguchi," Higher-order sampling, over sampling and digital filtering techniques for radio interferometry," IEICE Trans. Commun., E85-B, 9, pp1806-1816, 2002.
15. H.Kiuchi, "Parallel bit stream correlation system for very long interferometry," Radio Science, Vol.40, RS5013, doi: 10.1029/2005RS003282, 2005.
16. J.D.Romney, "4. Cross Correlators," Synthesis Imaging in Radio Astronomy II, ASP Conference Series, Vol. 180, 1999.

17. CORL-62.00.00.00-006-A-REP.
18. A.E.E.Rogers, A.T.Moffet, D.C.Backer and J.M.Moran,"Coherence limits in VLBI observation at 3-millimeter wavelength," Radio Science, vol.19, no.6, pp.1552-1560, Nov.1984.
19. ALMA-34.00.00.00.006-A-SPE
20. Y.Asaki, M.Saito, R.Kawabe, K.Morita, Y.Tamura, and B.Vila-vilaro, "Simulation series of a phase calibration scheme with water vapor radiometers for the Atacama Compact Array," ALMA memo 535.